REPORT DOCUMENTATION PAGE

Form Approved
OMB No. 0704-0188

1. Agency Use Only *(Leave blank).*	2. Report Date.	3. Report Type and Dates Covered.
	1990	Journal Article

4. Title and Subtitle.
A stable data-adaptive method for matched-field array processing in acoustic waveguides

5. Funding Numbers.
Program Element No. 61153N
Project No. 03105
Task No. 330
Accession No. DN255005

6. Author(s).
Charles L. Byrne, Ronald T. Brent, Christopher Feuillade, and Donald R. DelBalzo

7. Performing Organization Name(s) and Address(es).
Naval Oceanographic and Atmospheric Research Laboratory*
Stennis Space Center, MS 39529-5004

8. Performing Organization Report Number.
JA 244:033:89

9. Sponsoring/Monitoring Agency Name(s) and Address(es).
Naval Oceanographic and Atmospheric Research Laboratory*
Basis Research Management Office
Stennis Space Center, MS 39529-5004

10. Sponsoring/Monitoring Agency Report Number.
JA 244:033:89

11. Supplementary Notes.
*Formerly Naval Ocean Research and Development Activity

12a. Distribution/Availability Statement.
Approved for public release; distribution is unlimited.

12b. Distribution Code.

13. Abstract *(Maximum 200 words).*
Capon's maximum likelihood (ML) method has been used with some success in matched field processing for source range and depth estimation. One reason for the interest in the ML is that it is data adaptive; that is, it adapts to the actual noise field present rather than requiring an a priori estimate of the noise component for prewhitening. When modal noise is present the ML can become sensitive to any deviations from the unperturbed case (i.e., from the model) as would be introduced by phase errors or model parameter errors. Using a dimensionality-reduction procedure a more stable data adaptive method, the 'reduced' ML (RML), is obtained. The RML is compared here with the ML on simulated data from a 21-sensor array in a Pekeris waveguide supporting eight normal modes. Under modal noise conditions the RML provides a significant improvement over ML when phase errors occur. Although the deviation from the model considered here is that caused by phase errors, the nature of the perturbation is not important since the sensitivity of ML is not to any special type of perturbations.

14. Subject Terms.
(U) Shallow water; (U) Algorithms

15. Number of Pages.
10

16. Price Code.

17. Security Classification of Report.	18. Security Classification of This Page.	19. Security Classification of Abstract.	20. Limitation of Abstract.
Unclassified	Unclassified	Unclassified	SAR

A stable data-adaptive method for matched-field array processing in acoustic waveguides

Charles L. Byrne and Ronald T. Brent
Department of Mathematics, University of Lowell, Lowell, Massachusetts 01854

Christopher Feuillade
Syntek Engineering and Computer Systems Inc., 2 Crystal Park, Suite 600, 2121 Crystal Drive, Arlington, Virginia 22202

Donald R. DelBalzo
Naval Ocean Research and Development Activity, Stennis Space Center, Mississippi 39529-5004

(Received 14 August 1989; accepted for publication 11 January 1990)

Capon's maximum likelihood (ML) method has been used with some success in matched field processing for source range and depth estimation. One reason for the interest in the ML is that it is data adaptive; that is, it adapts to the actual noise field present rather than requiring an *a priori* estimate of the noise component for prewhitening. When modal noise is present the ML can become sensitive to any deviations from the unperturbed case (i.e., from the model) as would be introduced by phase errors or model parameter errors. Using a dimensionality-reduction procedure a more stable data adaptive method, the "reduced" ML (RML), is obtained. The RML is compared here with the ML on simulated data from a 21-sensor array in a Pekeris waveguide supporting eight normal modes. Under modal noise conditions the RML provides a significant improvement over ML when phase errors occur. Although the deviation from the model considered here is that caused by phase errors, the nature of the perturbation is not important since the sensitivity of ML is not to any special type of perturbation.

PACS numbers: 43.30.Wi, 43.30.Bp, 43.60.Gk

INTRODUCTION

A number of recent articles have considered the topic of matched field processing, in which the plane wave steering vector used in bearing estimation is replaced by a more complicated vector that models what appears at the array when there is a source at a particular range and depth in a waveguide.[1-5] Most published work to date deals with a range-independent propagation model and employs a normal mode representation of the pressure field. When a conventional matched filter approach to range-depth estimation is taken, the resulting ambiguity surface often contains several false peaks. To obtain smoother surfaces one can use various "mode space" beamforming methods[4,5]; recently, the use of Capon's maximum likelihood (ML) method[6,7] has also been considered.[2,3]

It has been shown for the plane waves case[8] that Capon's ML can become quite sensitive to deviations from the unperturbed model case in the presence of a correlated noise field, such as spherical isotropic noise with an oversampled array. For the more complicated case of normal mode propagation in a waveguide, the ML again exhibits sensitivity to perturbations in the data, particularly in the presence of modal noise. "Sector-focused stability" (SFS) was introduced in Ref. 8 to stabilize the ML in the plane wave case. The SFS involves the use of a square matrix whose size can be considerably less than the number of sensors, and therefore reduces computation cost and numerical errors while improving stability. When the philosophy behind SFS is applied to the case of normal mode propagation in a waveguide we obtain the "reduced" ML (RML).

To understand why the ML is unstable in the cases considered we examine the eigenvector/eigenvalue decomposition of the cross spectral matrix obtained from the data and expand the ML estimator as the reciprocal of a sum of terms, one for each eigenvector. Most of the terms in the denominator of the ML estimator will be zero at the correct range and depth, leading to a large peak in the ML estimator. When there are no phase errors, several terms in the sum vanish identically across the ambiguity surface. When phase errors are present these terms are slightly bigger than zero everywhere and the value of the denominator at the true range and depth increases, leading to a drop in peak height. By removing the offending small, but positive, terms one can restore the peak and stabilize the ML estimator; when so modified the estimator becomes the RML. It is not necessary to calculate each eigenvector and each term separately; a dimensionality-reduction procedure accomplishes this and avoids the inversion of the full-sized matrix as well.

The paper is organized as follows: Sec. I formulates the problem in mathematical language, presenting the normal mode model for the vector of pressure field samples, introducing the theoretical cross spectral matrix to be used throughout, and touching briefly on two linear estimators, the conventional matched filter method (CONV) and the mode space version of the conventional estimator, called here the modified conventional method (MCONV). In Sec. II we present Capon's ML method, discuss proper normali-

 0001-4966/90/062493-10$00.80

zation procedures, introduce the eigenvector/eigenvalue decomposition, and consider the source of the instability. In Sec. III we develop the RML and present alternate methods for its calculation. Section IV contains a discusion of our simulations and results. Section V contains comments and conclusions. We include three appendices. The first extends our discussion of the sensitivity problem to local normal mode models for the range-dependent case, and the second is concerned with similar sensitivity in the use of the parabolic approximation. The third appendix contains a mathematical derivation relevant to the normalization of the ML estimator.

I. FORMULATION AND BACKGROUND

We consider a vertical array of N sensors in an acoustic waveguide supporting $M < N$ discrete propagating modes. We shall be concerned here with the case studied by Buckingham,[9] the so-called "low-loss" situation, in which the main contribution to the ambient noise field is discrete modal propagation over long distances of acoustic energy due to independent, randomly distributed, surface sources (see also Kuperman and Ingenito[10]). For the case we consider here the single-snapshot, narrow-band, data vector $\mathbf{x}$ (N by 1) has the algebraic form

$$\mathbf{x} = a_0 U\mathbf{s} + U\boldsymbol{\gamma} + \boldsymbol{\eta} . \tag{1}$$

Here, U is the N by M matrix whose (n,m)th entry is $U_{n,m} = U_m(z_n)$, which is the evaluation, at the depth z_n of the nth sensor, of the mth mode amplitude function (see Kuperman and Ingenito,[10] p. 1990). The entries of $\mathbf{s}$ and (random vector) $\boldsymbol{\gamma}$ represent the excitation of the various mode amplitude functions by the signal and the aggregate noise sources, respectively. Also, a_0 is a complex Gaussian random amplitude and $\boldsymbol{\eta}$ is a random white (nonmodal) noise vector.

For the case of range-independent sound speed and density, and assuming cylindrical symmetry, the pressure field at depth z due to a single source at depth z_s and range r is given by

$$p(r,z_s,z) = \sum_{m=1}^{M} U_m(z) s_m(r,z_s) , \tag{2}$$

where the $U_m(z)$ are the samples, at the sensor depth z, of the mth modal eigenfunction that arises as a solution to the depth variable Sturm–Liouville boundary value problem,[11] and the $s_m(r,z_s)$ are the modal amplitudes given by

$$s_m(r,z_s) = U_m(z_s)\exp(ik_m r)(2\pi/k_m r)^{1/2} . \tag{3}$$

The matrix U has entries $U_{n,m} = U_m(z_n)$, where $z_1,\ldots,z_N$ are the depths of the N sensors and the vector $\mathbf{s}$ has the entries $s_m(r,z_s)$. Here, k_m^2 is the eigenvalue associated with the mth mode. The noise vector $U\boldsymbol{\gamma}$ represents modal noise created by the excitation of the modal structure by distributed independent sources of ambient acoustic energy, such as wave action on the surface and/or many range-separated surface ships (see Kuperman and Ingenito,[10] p. 1990).

When the sound speed or the density is range dependent, one can modify the normal-mode analysis to obtain a theory based on local normal-mode structure,[11,12] or use a parabolic approximation.[13] In either case the model given by Eq. (1) applies. We consider these two approaches to the range-dependent case in Appendices A and B.

For $\mathbf{x}$ given by Eq. (1), the cross-spectral matrix (CSM) is $R = \langle \mathbf{x}\mathbf{x}^H \rangle$, with H denoting conjugate transposition and $\langle\ \rangle$ time averaging; R is the average, over the available snapshots, of the dyad matrices $\mathbf{x}\mathbf{x}^H$, and is given (approximately) by

$$R = \mathrm{var}(a_0) U\mathbf{s}_0\mathbf{s}_0^H U^H + UQU^H + \rho^2 I , \tag{4}$$

where Q is the CSM associated with the modal noise field (i.e., $Q = \langle \boldsymbol{\gamma}\boldsymbol{\gamma}^H \rangle$) and ρ^2 is the white noise power. The matrix Q may or may not be a diagonal matrix. This depends on the geometric distribution of random sources comprising the ambient noise field, and does not follow solely from the independence of each of these random sources.[9,14] The matrix Q is diagonal in the Kuperman–Ingenito development (Ref. 10, p. 1991) because of the assumption made in their work that the spatial coherence of the noise depends only on separation. The matrix UQU^H plays the same role as K_c in Baggeroer *et al.*[2]

We shall adopt the following model for the CSM R:

$$R = \beta^2 U\mathbf{s}_0\mathbf{s}_0^H U^H + \sigma^2 UU^H + \rho^2 I . \tag{5}$$

This represents a single source $\mathbf{s}_0$, a correlated (modal) noise component $UQU^H (Q = \sigma^2 I)$, and a white noise component $\rho^2 I$. More general models, which include a second (interfering) source, have also been considered,[2] but Eq. (5) will be sufficient for our purposes. It is a relatively high level of the $\sigma^2 UU^H$ term that will be of importance here. That Q be diagonal is not crucial to our analysis; only that Q have full rank M.

The first step in any matched-field approach to estimating $\mathbf{s}_0$ is to construct, for each potential source vector $\mathbf{s} = \mathbf{s}(r,z)$ (where r and z are range and depth), the vector $\mathbf{p}(r,z) = U\mathbf{s}(r,z)$ that the array would have received. This can be done through the use of complex computer models of the propagation, such as parabolic approximation routines,[13] or by employing the matrix U directly if it can be obtained from a (local) normal-mode model.[12] The conventional estimator is essentially the matched filter:

$$\mathrm{CONV}(r,z) = \mathbf{p}(r,z)^H R\mathbf{p}(r,z) , \tag{6}$$

and the plot of $\mathrm{CONV}(r,z)$ over ranges and depths of interest is referred to as the ambiguity surface. A detailed discussion of the conventional approach to matched field processing is given in Ref. 2. An alternative method involving, for the normal-mode case, the passage to "mode space"[4,5] is the following modified conventional method:

$$\mathrm{MCONV}(r,z) = \mathbf{s}(r,z)^H (U^H U)^{-1} U^H R U (U^H U)^{-1} \mathbf{s}(r,z) . \tag{7}$$

It can be shown that MCONV is the optimal linear processor for minimizing sidelobe structure if the distribution of potential sources resembles a noise component of the form $\sigma^2 UU^H$. Equivalently, MCONV is the optimal linear procedure to maximize array gain against noise having the form $\sigma^2 UU^H$.

As with the plane wave case, when the noise is not white the CONV method is not optimal and the optimal procedure

then involves a prewhitening. This prewhitening requires knowledge of the actual noise-only cross-spectral matrix. Since such knowledge is usually not available one might prefer to use a method that adapts to whatever the noise component happens to be, rather than relying on an *a priori* model of the noise; the ML method is such a data-adaptive method.

II. CAPON'S MAXIMUM LIKELIHOOD METHOD

Capon's maximum likelihood (ML) method is a nonlinear estimator in that the inverse of R is required and that its resolving capability increases with SNR. For moderate levels of SNR it has better resolution than CONV. It is convenient to use because it does not require prior knowledge of the ambient noise (it adapts to whatever noise is present) and can be used with any array geometry. When applied to matched field processing it often presents a less ambiguous ambiguity surface than CONV. The derivation of ML can be extended without difficulty from the plane wave case to that of more complicated propagation in a waveguide and it is this extended ML that we consider here.

For R as in Eq. (4) and $\mathbf{p}(r,z) = U\mathbf{s}(r,z)$, Capon's ML method leads to the maximum likelihood estimator

$$\mathrm{ML}(r,z) = 1/[\mathbf{p}(r,z)^{H} R^{-1} \mathbf{p}(r,z)]. \tag{8}$$

A detailed discussion of this estimator and its application to acoustic waveguide array processing is to be found in Ref. 2. Our treatment here is different in that we are concerned with the effects of a relatively high level of modal noise. We find it helpful to analyze the ML estimator in terms of the eigenvectors and eigenvalues of R. The matrix R is Hermitian positive definite and so has positive eigenvalues $\lambda_1 \geq \lambda_2 \geq \cdots \geq \lambda_N > 0$ and associated orthogonal eigenvectors $\mathbf{z}_1,\ldots,\mathbf{z}_N$, normalized to have norm equal to one. It follows from the form for R given in Eq. (4) that $\lambda_{M+1} = \cdots = \lambda_N = \rho^2$ and that, for $n = M+1,\ldots,N$, $\mathbf{z}_n$ is orthogonal to the columns of U.[15a] If we now rewrite the ML estimator as

$$\mathrm{ML}(r,z) = \left(\sum_{n=1}^{N} \lambda_n^{-1} |\mathbf{z}_n^{H} \mathbf{p}(r,z)|^2 \right)^{-1}, \tag{9}$$

we see that the terms from $n = M+1$ to N are identically equal to zero for all $\mathbf{p}(r,z)$, so they play no role in the ML estimator and the denominator of ML reduces to a sum over $n = 1,\ldots,M$. When phase errors are present the eigenvectors of R are altered and the terms corresponding to $n = M+1,\ldots,N$ do not vanish identically, causing the ML estimator to degrade. If we eliminate these last $N - M$ terms we obtain a new estimator, which we call the "reduced" ML (RML).

In plane wave array processing the steering vectors [analogous to our $\mathbf{p}(r,z)$] have constant norm, so no normalization of ML is required. For normal mode (or more general) models $\mathbf{p}(r,z)^{H}\mathbf{p}(r,z)$ is not constant and for that reason it is common to calculate a normalized ML. In our case this would involve multiplying (8) by $\mathbf{p}(r,z)^{H}\mathbf{p}(r,z)$ or, equivalently, replacing each $\mathbf{p}(r,z)$ by $\mathbf{p}(r,z)/[\mathbf{p}(r,z)^{H}\mathbf{p}(r,z)]^{1/2}$. We feel that this is not a reasonable procedure and offer analytic argument in favor of a different normalization.

For the situation considered here the noise is primarily modal so that, in the absence of a signal, the CSM R would have the form $R = UU^{H} + \epsilon I$, for some small $\epsilon > 0$. In Appendix C we show that as ϵ goes to 0 the ML ambiguity surface for this R goes to $\mathbf{s}(r,z)^{H}\mathbf{s}(r,z)$. We choose therefore to normalize our ML surfaces by dividing by $\mathbf{s}(r,z)^{H}\mathbf{s}(r,z)$, instead of by $\mathbf{p}(r,z)^{H}\mathbf{p}(r,z)$. This change in normalization is important when there is a sizeable modal noise component. Figures 1 and 2 illustrate the ML estimator for R as in (5), normalized by dividing by $\mathbf{p}(r,z)^{H}\mathbf{p}(r,z)$ and by $\mathbf{s}(r,z)^{H}\mathbf{s}(r,z)$, respectively.

III. THE "REDUCED" MAXIMUM LIKELIHOOD METHOD (RML)

The "reduced" maximum likelihood estimator (RML) agrees with Eq. (9) except that the sum is over the first M terms only:

$$\mathrm{RML}(r,z) = \left(\sum_{n=1}^{M} \lambda_n^{-1} |\mathbf{z}_n^{H} \mathbf{p}(r,z)|^2 \right)^{-1}. \tag{10}$$

We shall compare ML with RML in our simulations and observe the extent to which ML degrades when phase errors are present. To compute RML it is not necessary to obtain explicitly the eigenvalues and eigenvectors of R; in fact, RML can be obtained from the matrix used in the MCONV.

The passage to "s space" that occurs in calculating the MCONV involves the transformation of R to $T = (U^{H}U)^{-1}U^{H}RU(U^{H}U)^{-1}$ and the transformation of the "potential source" (or "steering") vectors $\mathbf{p} = \mathbf{p}(r,z)$ to $\mathbf{s} = \mathbf{s}(r,z) = (U^{H}U)^{-1}U^{H}\mathbf{p}(r,z)$. Applying the usual "maximum likelihood" approach of Capon, we are led to consider the estimator $1/\mathbf{s}^{H}T^{-1}\mathbf{s}$, which as we shall show, is equivalent to the RML.

To show equivalence of the two estimators we begin with the eigenvalue–eigenvector decomposition of R

$$R = \sum_{n=1}^{M} \lambda_n \mathbf{z}_n \mathbf{z}_n^{H}. \tag{11}$$

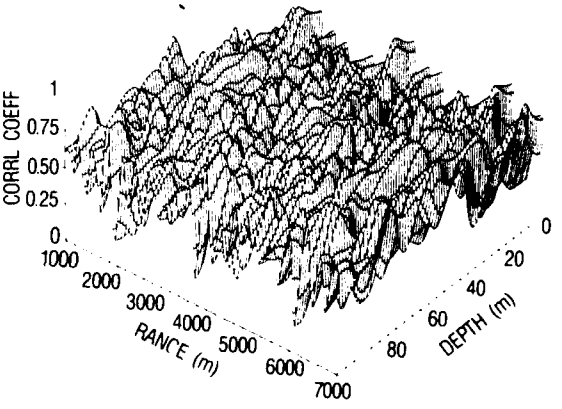

FIG. 1. Ambiguity surface produced using ML estimator for Pekeris waveguide environment. The level of white noise is −30 dB (i.e., a signal to white noise ratio of 30 dB). The level of modal noise is 20 dB (i.e., a signal to modal noise ratio of −20 dB). The steering vectors are normalized so that $\mathbf{p}(r,z)^{H}\mathbf{p}(r,z) = 1$, for all r,z.

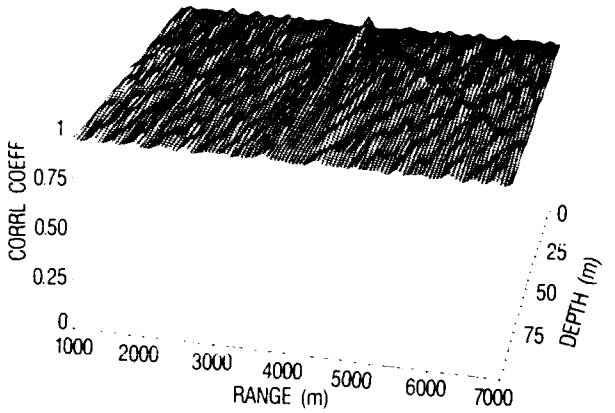

FIG. 2. Ambiguity surface produced using ML estimator for identical environmental and noise conditions as in Fig. 1. The steering vectors are normalized so that $\mathbf{s}(r,z)^{H}\mathbf{s}(r,z) = 1$, for all r,z.

Since $\mathbf{z}_n$ is orthogonal to the columns of U for $n \geqslant M+1$, the $\mathbf{z}_n$ for $n = 1,\ldots,M$ must be in the linear span of these same columns,[15a] that is, $\mathbf{z}_n = U\mathbf{a}_n$ for some $\mathbf{a}_n$ $(n \leqslant M)$. Hence,

$$U^{H}RU = \sum_{n=1}^{M} \lambda_n U^{H}\mathbf{z}_n\mathbf{z}_n^{H}U$$

$$= \sum_{n=1}^{M} \lambda_n (U^{H}U)\mathbf{a}_n\mathbf{a}_n^{H}(U^{H}U)\,. \qquad (12)$$

Then with $W = (U^{H}U)^{1/2} = W^{H}$ we have

$$W^{-1}U^{H}RUW^{-1} = \sum_{n=1}^{M} \lambda_n W\mathbf{a}_n\mathbf{a}_n^{H}W^{H}\,. \qquad (13)$$

Since $(W\mathbf{a}_n)^{H}(W\mathbf{a}_k) = \mathbf{a}_n^{H}W^{H}W\mathbf{a}_k = \mathbf{a}_n^{H}U^{H}U\mathbf{a}_k = \mathbf{z}_n^{H}\mathbf{z}_k$ it follows that $\{W\mathbf{a}_n,\ n = 1,\ldots,M\}$ is an orthogonal set, in which case

$$(W^{-1}U^{H}RUW^{-1})^{-1} = W(U^{H}RU)^{-1}W$$

$$= \sum_{n=1}^{M} \lambda_n^{-1}W\mathbf{a}_n\mathbf{a}_n^{H}W^{H}\,. \qquad (14)$$

By eliminating the W from the left and the right one obtains

$$(U^{H}RU)^{-1} = \sum_{n=1}^{M} \lambda_n^{-1}\mathbf{a}_n\mathbf{a}_n^{H}\,. \qquad (15)$$

Since $\mathbf{s} = \mathbf{s}(r,z) = (U^{H}U)^{-1}U^{H}\mathbf{p}(r,z)$ we have,

$$\mathbf{s}(r,z)^{H}T^{-1}\mathbf{s}(r,z) = \mathbf{p}(r,z)^{H}U(U^{H}RU)^{-1}U^{H}\mathbf{p}(r,z)\,. \qquad (16)$$

Using Eq. (15) in Eq. (16) we have

$$\mathbf{s}(r,z)^{H}T^{-1}\mathbf{s}(r,z) = \sum_{n=1}^{M} \lambda_n^{-1}\mathbf{p}(r,z)^{H}U\mathbf{a}_n\mathbf{a}_n^{H}U^{H}\mathbf{p}(r,z)$$

$$= \sum_{n=1}^{M} \lambda_n^{-1}|\mathbf{z}_n^{H}\mathbf{p}(r,z)|^2\,. \qquad (17)$$

Hence,

$$\mathrm{RML} = [\mathbf{s}^{H}(r,z)T^{-1}\mathbf{s}(r,z)]^{-1}, \qquad (18)$$

and the RML estimator has precisely the same form as the ML estimator (8). We note that in order to calculate RML we need only invert the single matrix $U^{H}RU$ (16), which is M by M.

From the above calculations we see that RML can be calculated as

$$\mathrm{RML}(r,z) = [p(r,z)^{H}U(U^{H}RU)^{-1}U^{H}p(r,z)]^{-1}. \qquad (19)$$

The matrix $(U^{H}RU)$ to be inverted can be ill-conditioned and it is safer to orthogonalize U first. We can use "QR factorization"[15b] to write $U = VX$, where V is an N by M matrix with M orthogonal columns of unit length and X is an upper triangular matrix; this is essentially Gram–Schmidt orthogonalization in matrix language. We then have $V^{H}V = I$, and replacing U with VX in (19) leads to

$$\mathrm{RML}(r,z) = [p(r,z)^{H}V(V^{H}RV)^{-1}V^{H}p(r,z)]^{-1}. \qquad (20)$$

The matrix $V^{H}RV$ will be better conditioned than $U^{H}RU$ generally, and so more accurately inverted.

We see from Eqs. (8) and (9) that the ML estimator will show a peak at the true value $\mathbf{p} = \mathbf{p}_0 = U\mathbf{s}_0$ provided that the denominator is close to zero for $\mathbf{p} = \mathbf{p}_0$ and larger for neighboring values. The information about the signal is then carried by the (near) nulls of the functions $|\mathbf{z}_n^{H}\mathbf{p}(r,z)|^2$, for $n = 2,\ldots,N$. When the denominator is perturbed by the addition of small but nonzero quantities these (near) nulls are disturbed, with the result being the loss of the peak at the true signal location. This is what happens when the terms corresponding to $n = M+1,\ldots,N$ are no longer identically zero, due to the presence of phase errors. In our simulations we compare the performance of the ML and the RML for varying amounts of phase error. Before we pass to the simulations it will be instructive to examine the behavior of the ML estimator in one special case, in which $U^{H}U = I$.

With $U^{H}U = I$ we have $\lambda_1 = \alpha^2 + \sigma^2 + \rho^2$, $\lambda_2 = \cdots = \lambda_M = \sigma^2 + \rho^2$, where the signal power is $\alpha^2 = \beta^2\mathbf{s}_0^{H}\mathbf{s}_0$. We can then write the ML estimator as

$$\mathrm{ML} = \left(\lambda_1^{-1}|\mathbf{z}_1^{H}\mathbf{p}|^2 + (\sigma^2+\rho^2)^{-1}\sum_{n=2}^{M}|\mathbf{z}_n^{H}\mathbf{p}|^2 + \rho^{-2}\sum_{n=M+1}^{N}|\mathbf{z}_n^{H}\mathbf{p}|^2\right)^{-1}. \qquad (21)$$

As the α^2 gets larger the value of λ_1^{-1} gets smaller, so the first term in the denominator gets smaller, making the (near) nulls of the remaining terms more significant and the peak of the ML estimator more visible. For smaller values of α^2, however, the first term contributes a sizable nonzero quantity to the denominator, causing the (near) nulls of the remaining terms to become less significant and the peak in the ML estimator to drop; this is the reason for the dependence of resolution on SNR.

Holding α and ρ fixed, let us consider the effects of raising σ. As σ is changed, the eigenvectors $\mathbf{z}_n$, $n = 1,\ldots,M$ change, while those for $n = M+1,\ldots,N$ do not. If σ^2 is small compared to $\alpha^2+\rho^2$, for $n = 2,\ldots,M$, the values of $|\mathbf{z}_n^{H}\mathbf{p}(r,z)|^2$ will be nearly zero for (r,z) corresponding to the true source parameters, but as σ increases, these (near) nulls will weaken and become less distinguished from neighboring values. In addition, as σ increases, $\lambda_1^{-1} = (\alpha^2+\sigma^2+\rho^2)^{-1}$ becomes more like $\lambda_2^{-1} = \cdots = \lambda_M^{-1} = (\sigma^2+\rho^2)^{-1}$, increasing the (unwanted) contribution from the first term in the denominator of Eq. (21). The overall effect is to make

the (near) null in the signal direction more shallow, to raise the background noise level and to increase sensitivity to the presence of the third term in the denominator of Eq. (21).

IV. RESULTS

In this section we investigate, by means of computational simulation within an assumed shallow-water acoustic environment, the behavior of both ML and RML estimators as they respond to varying amounts of phase error applied randomly to the elements of the hydrophone array. The geoacoustic environmental model used here is the two-layered liquid half-space model of Pekeris.[16,17] Even though the simplicity of the Pekeris model limits its general applicability, it does possess features that are very similar to at least one shallow-water environment in which matched-field experiments have been performed.[18] In this case, the water sound-speed profile was almost isospeed, and a thick sandy sediment layer was present, which carried no shear waves and therefore behaved like a liquid. The Pekeris model is also a widely used and well-understood standard model. It should describe most of the acoustic characteristics of general shallow-water waveguides. Since the acoustic wavefunctions within the waveguide are calculated analytically, without need for recourse to numerical techniques, the calculation of the pressure field vectors $\mathbf{p}$, the transformation matrices U and the modal amplitude vectors $\mathbf{s}$ is greatly facilitated. This makes the transformation from R to T, and therefore the calculation of the RML estimator (18), a relatively simple matter.

The Pekeris model consists of a shallow isospeed water layer of uniform density overlying a faster, isospeed, semi-infinite fluid bottom of uniform (and usually higher) density. For a full description of the general Pekeris model, the reader is referred to a standard text (e.g., Ref. 17). In this work the water depth is 100 m, the sound speed in the water and sediment is 1500 and 1621.6 m/s, respectively, and the sediment/water density ratio is 1.772. The acoustic source has a frequency of 150 Hz, which leads to the establishment of eight propagating modes in this waveguide. The source was placed at a range of 4000 m from the array at a depth of 10 m. A vertical hydrophone array consisting of 21 evenly spaced hydrophones is placed to sample the central 50 m of the water column.

The difference in order of the modal and hydrophone space cross-spectral matrices here does not lead to any undue computational problems in transforming from one processing space to the other. Since the array spans only 50% of the water column the matrix $U^{\prime\prime}U \neq I$, and its eigenvalues will typically not have the distribution described by (21). However, many of the broad features of the eigenvalue distribution will be similar to (21), which may frequently serve as a basis for interpreting the phenomena observed when the noise levels are varied.

White noise is introduced into the system by adding an appropriate constant [i.e., ρ^2 in Eq. (5)] to every diagonal element of the cross-spectral matrix in hydrophone space R. The value of ρ^2 is determined by scaling against the mean power detected on the hydrophones (equivalent to the mean diagonal element of R). Modal noise is introduced in a similar way, by adding a constant σ^2 to the diagonal elements of the modal space cross-spectral matrix T. The value of σ^2 is determined by scaling the diagonal elements of $\sigma^2 UU^{\prime\prime}$ against the mean power detected on the hydrophones. In these simulations the acoustic source level is held steady so that the field detected at the hydrophone array due to the source remains constant. The values of ρ^2 and σ^2 are then adjusted to achieve the desired levels of white noise and modal noise, respectively. We will quantify the values of ρ^2 and σ^2 in terms of their dB level above (+) or below (−) the signal level. Note that this method of quantifying the noise levels (which is convenient and helpful here) is the opposite of that usually adopted. Thus, a modal noise level of −10 dB would correspond to a signal to modal noise ratio of +10 dB. The same applies to the relationship between the level of white noise and the signal to white noise ratio.

In order to provide a means of quantifying the roughness of the ambiguity surfaces, and a measure of peak resolution, the peak value (P), mean background level (μ), and standard deviation of the background (ν) are calculated for each surface. The mean background level is calculated by excluding a small interval around the peak. Two measures of peak-to-background resolution are used.[19,20] These are PBR1 $= (P-\mu)/\mu$ and PBR2 $= (P-\mu)/\nu$. We do not infer statistical behavior from these quantities, but merely use them as indicators of "goodness" of the surfaces.

Phase errors are introduced into the system in the following manner. First the *maximum* phase error is specified, say θ degrees. (We refer to this number simply as the "random phase error" or RPE.) Then a diagonal matrix D is formed:

$$D = \mathrm{diag}[\exp(i\phi_n)], \quad n = 1,\ldots,N, \tag{22}$$

where the ϕ_n are independent random variables uniformly distributed between $-\theta$ and $+\theta$. Then the CSM R is replaced by $\bar{R} = DRD^{\prime\prime}$.

Before we begin to investigate the stability of the ML and RML estimators to phase error, we will reconsider briefly the question of estimator normalization first raised in Sec. II. The importance of this question may be illustrated very clearly if we consider a case where white noise is introduced at a low level compared with the signal ($\rho^2 = -30$ dB), while the level of modal noise is considerably higher than the signal ($\sigma^2 = 20$ dB). No phase errors are yet introduced. In Fig. 1 we see the ambiguity surface obtained by using the summation expression (9) for the ML estimator with these inputs. In this example the steering vectors $\mathbf{p}(r,z)$ are normalized to have unity norm [i.e., $\mathbf{p}(r,z)^{\prime\prime}\mathbf{p}(r,z) = 1$, for all r,z]. Figure 1 indicates that, for the noise level inputs detailed above, this normalization procedure applied to the ML estimator results in a highly erratic ambiguity surface. A ridge can be seen close to the input source position (10-m depth and 4000-m range), but it is masked by numerous sidelobes. Several of these have greater intensity than the signal peak. Clearly, reliable and unambiguous estimation is not possible on this surface.

Rather than normalizing the $\mathbf{p}(r,z)$ to have unity norm, we normalize so that their corresponding *modal* vectors $\mathbf{s}(r,z)$ have unity norm [i.e., $\mathbf{s}(r,z)^{\prime\prime}\mathbf{s}(r,z) = 1$, for all r,z].

With this choice of normalization the ML estimator would give a flat ambiguity surface, in the noise-only case, if the CSM is $R = UU^{\prime\prime}$. If we again use the summation expression (9) to recalculate the ML ambiguity function for the $\rho^2 = -30$ dB, $\sigma^2 = 20$ dB case discussed in the previous paragraph, we obtain the surface in Fig. 2. It must be stressed here that Figs. 1 and 2 have been calculated using an identical algorithm [i.e., Eq. (9)] with identical inputs. The *only* difference between them is the way the steering vectors $\mathbf{p}(r,z)$ have been normalized. In fact, since the vector $\mathbf{s}(r,z)$ used in the calculation of the RML estimator (18) is always normalized so that $\mathbf{s}(r,z)^{\prime\prime}\mathbf{s}(r,z) = 1$ (for all r,z), and since the summation for the RML estimator (10) is equivalent to the summation for the ML estimator (9) (when the terms for $n = M+1,\ldots,N$ are zero), we have the surprising result that the ML estimator (9) and the RML estimator (10) are equivalent *except* for the way the steering vectors $\mathbf{p}(r,z)$ are normalized in the two cases. However, this is *not* true in the presence of phase errors, or any other factors, which cause the terms for $n = M+1,\ldots,N$ in the ML summation (9) to become nonzero, as we shall see later.

If we inspect Fig. 2 we see that the ambiguity surface contains an unambiguous primary peak at the input source location (10-m depth and 4000-m range); but it is most notable for two other features. The first is the lack of contrast between peaks and valleys on the surface itself; and the second is the high overall level of the surface, which is compressed into the top 10% of the available range of estimator values. The reason for this may be seen by inspection from Eqs. (9) and (21). The eigenvalues λ_n appearing in the summation on the rhs of Eq. (9) take the values $\lambda_1 \simeq \alpha^2 + \sigma^2 + \rho^2$; $\lambda_2,\ldots,\lambda_M \simeq \sigma^2 + \rho^2$; $\lambda_{M+1},\ldots,\lambda_N = \rho^2$; and since $\sigma^2 \gg \alpha^2 + \rho^2$ all of these eigenvalues are dominated by σ^2 and those for $n = 1,\ldots,M$ have similar magnitude. Now, as described earlier, information about the signal in ML processing is carried by the (near) nulls of the functions $|\mathbf{z}_n^{\prime\prime}\mathbf{p}(r,z)|^2$ (for $n = 2,\ldots,M$) in the denominator of Eq. (9) (the terms from $n = M+1$ to N are identically equal to zero for all $\mathbf{p}(r,z)$, so they play no role in the ML estimator). Now each of the nonzero terms is multiplied by a factor $\simeq 1/\sigma^2$. When σ^2 is large (as here) this factor tends to make them small over the whole range of $\mathbf{p}(r,z)$ rather than at just the source position and, because of the similarity of the eigenvalues for $n = 1,\ldots,M$ of comparable magnitude to the source term $\lambda_1^{-1}|\mathbf{z}_1^{\prime\prime}\mathbf{p}(r,z)|^2$. This decreases the reciprocal effect of the nulls at the source location and leads to the shallow relief of the details on the surface and its high overall background level. Although the surface in Fig. 2 is very flat and has a high background due to the large amount of modal noise, it does unambiguously indicate the presence and position of the source and is much more useful than Fig. 1. The reason for this is that it has been produced using a normalization procedure for the steering vectors which is optimized for the presence of modal noise. Since we will be considering cases, in our later simulations, where modal noise predominates over white noise, we will use the $\mathbf{s}(r,z)^{\prime\prime}\mathbf{s}(r,z)$ normalization throughout.

We will now proceed to consider the effects of phase error. We will be concerned here with a case where white noise is introduced at a low level compared to the signal ($\rho^2 = -30$ dB), while modal noise is considerably higher but still lower than the signal ($\sigma^2 = -10$ dB). In Fig. 3 we see the ambiguity surface obtained using the ML estimator (9) for these input noise levels with zero RPE on the hydrophones. This surface contains an unambiguous primary peak at the true source location (10-m depth and 4000-m range). The peak is extremely well resolved against all the sidelobes present which are minimal in intensity. As mentioned earlier, the terms for $n > M+1$ in the summation (9) should be identically zero for all $\mathbf{p}(r,z)$ when no phase errors are present, so that in this case ML and RML are equivalent to each other. Explicit calculation of the RML (17) for the same input conditions confirms that this is indeed the case. The RML produces an ambiguity surface identical to that of Fig. 3.

The reason for the high peak resolution on the surface in Fig. 3 may be seen by inspection of Eqs. (9) and (21). The eigenvalues λ_n appearing in the summation on the rhs of (9) take the values $\lambda_1 \simeq \alpha^2 + \sigma^2 + \rho^2$; $\lambda_2,\ldots,\lambda_M \simeq \sigma^2 + \rho^2$; and $\lambda_{M+1},\ldots,\lambda_N = \rho^2$. Since $\alpha^2, \sigma^2 \gg \rho^2$ we may further approximate these as $\lambda_1 = \alpha^2 + \sigma^2$; $\lambda_2,\ldots,\lambda_M \simeq \sigma^2$; $\lambda_{M+1},\ldots,\lambda_N = \rho^2$. Passing to Eq. (21) we recall that in ML information about the signal is carried by the nulls of the functions $|\mathbf{z}_n^{\prime\prime}p(r,z)|^2$, for $n = 2,\ldots,N$. In our case here these functions are identically zero for $n > M+1$ for all $\mathbf{p}(r,z)$ so we are really interested only in the nulls of the terms for $n = 2,\ldots,M$. In (21) we see that $\alpha^2 > \sigma^2$ and therefore $\lambda_1^{-1} < \lambda_n^{-1}$ $(n = 2,\ldots,M)$, making the first term in the denominator small and the nulls of the remaining terms more significant. This leads to the pronounced signal peak observed on the surface.

Let us now consider the effect of introducing phase errors onto the hydrophones. Figure 4 shows the ambiguity surface produced using ML when the RPE is 30 deg. We see immediately that a lot of degradation has taken place. Although the signal peak may still be observed at this point, it is now dominated by the sidelobe structure and may no longer be unambiguously resolved. The reason for this loss of performance is primarily due to the inclusion of the terms for

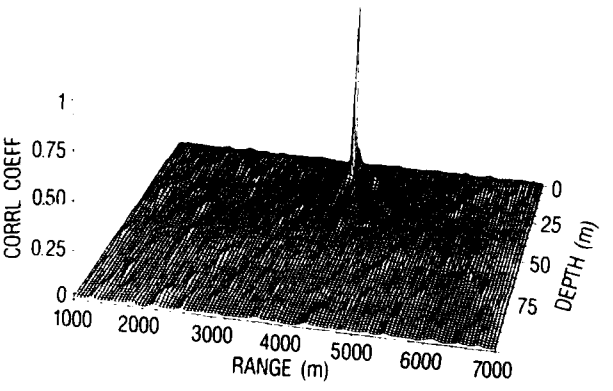

FIG. 3. Ambiguity surface produced using ML estimator for Pekeris waveguide environment. The level of white noise is -30 dB (i.e., a signal to white noise ratio of 30 dB). The level of modal noise is -10 dB (i.e., a signal to modal noise ratio of 10 dB). The RPE is 0 deg.

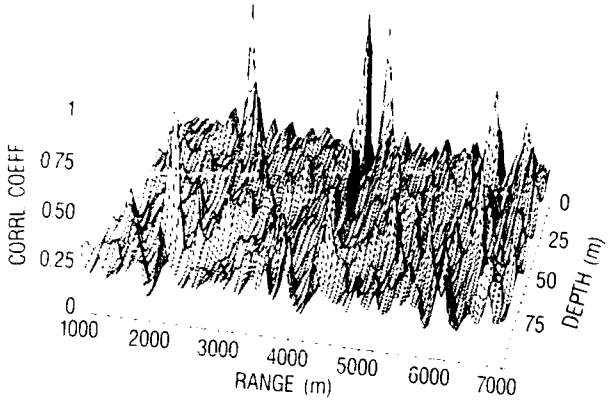

FIG. 4. Ambiguity surface produced using ML estimator for identical environmental and noise conditions as in Fig. 1. The RPE is 30 deg.

$n \geqslant M + 1$ in the summation for the ML estimator (9). With no phase errors these terms are identically zero, as we have seen. However, the introduction of phase errors into the CSM R, while leaving the eigenvalues λ_n unchanged, gives rise to arbitrary rotation of the eigenvectors $\mathbf{z}_n$ in the vector space of R. The projections of the steering vectors $\mathbf{p}(r,z)$ along the eigenvectors $\mathbf{z}_n$ ($n \geqslant M + 1$) then become nonzero. Although these projections may be relatively small their effect upon the summation in (9) is amplified by the λ_n^{-1} factor by which they are multiplied. We remember from (21) that for $n \geqslant M + 1$, $\lambda_n \cong 1/\rho^2$. Now ρ is the level of white noise, which in our case is low (-30 dB). Therefore $1/\rho^2$ is a large coefficient that can greatly exaggerate the contribution of the $n \geqslant M + 1$ terms to the summation, even when the RPE is comparatively small. Using the same environmental and noise conditions, we plot in Fig. 5 the percentage contribution to the summation in the denominator of the ML expression (9), when r and z are correct, due to the $n \geqslant M + 1$ terms. We see that the contribution rises rapidly as the phase error increases. It reaches 50% with an RPE of 35 deg and 95% with an RPE of only 80 deg. It asymptotically approaches 100% thereafter. With this in mind it is easy to understand how the sidelobe structure of the surface is enhanced by the presence of the extra, nonzero terms in the ML summation (9), and the stability of the estimator correspondingly decreased.

The RML estimator overcomes this problem of instability due to phase error by omitting the terms for $n \geqslant M + 1$ from the summation. Some errors will still be present due to the changes in the projections of the steering vectors $\mathbf{p}(r,z)$ along the eigenvectors $\mathbf{z}_n$ for $n \leqslant M$, as these are also rotated in the vector space due to the phase errors. However, this effect is much smaller and allows the RML estimator to remain stable to considerably higher degrees of phase error. Figure 6 shows the ambiguity surface obtained using the RML estimator with an RPE of 30 deg (cf. Fig. 4). Unlike the ML case, the signal peak is still unambiguously localized and sharply resolved against the sidelobe background. For this particular set of environmental and noise conditions, the RML estimator remains stable up to an RPE of 85 deg, when the sidelobes finally overcome the signal peak and the estimator fails. This represents a remarkable improvement over ML. Reference back to Fig. 5 shows that for an RPE of 85 deg the $n \geqslant M + 1$ terms contribute more than 95% to the ML summation (9). This is all simply avoided by using the RML.

Figure 7 displays the variation in PBR1 and PBR2 as a function of RPE for the ML and RML estimators. The environmental and noise conditions are unchanged from the previous examples. If we individually compare the PBR1 and PBR2 curves for the two cases we see that, by both measures, the RML estimator consistently outperforms the ML estimator throughout the range of RPE values investigated, except by a small amount within an interval between 0 and 15 deg. As the RPE is increased the ML estimator deteriorates very rapidly. The ML curves terminate at an RPE of 30 deg, beyond which the signal peak cannot be resolved. The RML curves also indicate a deterioration in performance, but at a much more moderate rate. As discussed above, the RML continues to provide accurate and robust localization estimates up to an RPE of 85 deg.

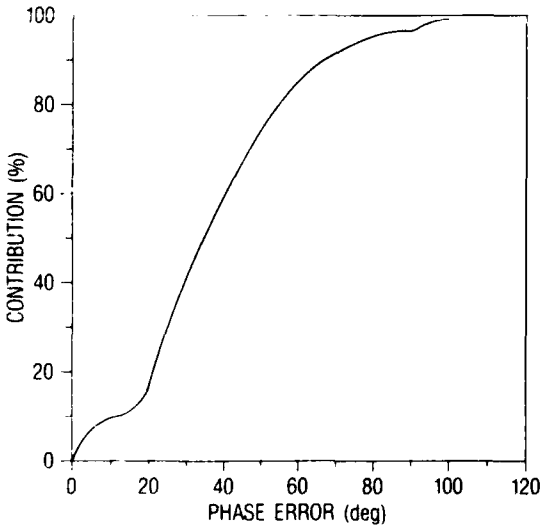

FIG. 5. Percentage contribution of $n \geqslant M + 1$ terms to summation in the denominator of expression (9) for the ML estimator. The environmental and noise conditions are those of the previous examples.

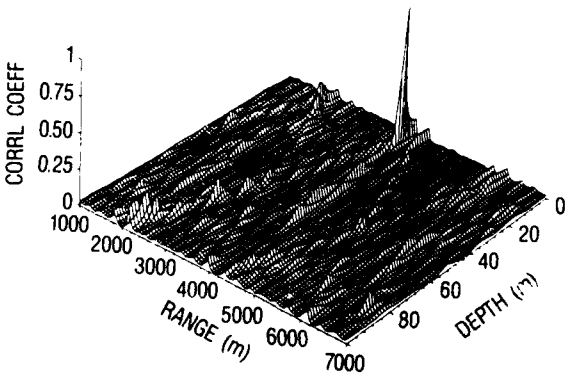

FIG. 6. Ambiguity surface produced using RML estimator for identical environmental and noise conditions as in Figs. 1 and 2. The RPE is 30 deg.

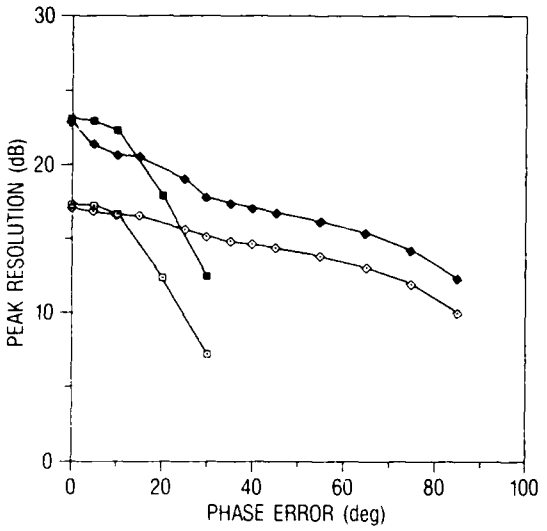

FIG. 7. Variation of PBR1 and PBR2 as functions of RPE for both ML and RML estimators. The environmental and noise conditions are those of the previous examples. The four curves are: (a) RML(PBR2)—shaded diamonds; (b) RML(PBR1)—unshaded diamonds; (c) ML(PBR2)—shaded squares; (d) ML(PBR1)—unshaded squares.

V. CONCLUSIONS

A modification of the data adaptive maximum likelihood (ML) method is presented that shows substantially improved stability in matched field processing for source localization. Instabilities in the ML estimator arise from phase errors in the signals received at the hydrophone array. These may be caused by a number of physical and environmental factors. We simulate them here by introducing random phase errors at the hydrophones. Applying the eigenvector/eigenvalue decomposition of the cross-spectral matrix R, the ML estimator is expanded as the reciprocal of a sum of terms, one corresponding to each eigenvector. In theory, most of these terms should be zero when the source has been correctly located, leading to a peak in the estimator. Due to perturbations in R caused by the phase errors, however, terms that should be zero across the entire ambiguity surface are not, leading to a drop in peak level. By removing these erroneous terms the estimator may be stabilized. We term the new estimator that results from this procedure the "reduced maximum likelihood" or RML estimator. Dimensionality reduction procedures are used to calculate the RML, avoiding inversion of the full-sized matrix or the calculation of eigenvalues.

Using a Pekeris waveguide model, simulations of acoustic propagation from a single source to a 21-hydrophone receiving array were used to examine the RML and ML estimators. In our particular model the waveguide supports eight modes and application of the RML estimator reduces the full problem of dimension 21 to one of dimension 8. Considering an environment with a large amount of modal noise (the signal to modal noise ratio is -20 dB) and little white noise (the signal to white noise ratio is 30 dB), it is found that using an ML estimator which is optimized for the presence of modal noise (by performing an appropriate normalization of the steering vectors) produces a far superior and more useful ambiguity surface than using an ML estimator which is optimized for the presence of white noise. In the absence of phase errors the ML and RML estimators are equivalent apart from the steering vector normalization schemes they employ.

In the case of an environment with a significant amount of modal noise (the signal to modal noise ratio is 10 dB) and little white noise (the signal to white noise ratio is 30 dB) the two methods are compared as they respond to increasing degrees of phase error introduced on the hydrophones. The results obtained clearly demonstrate the superiority of the RML estimator over the ML estimator. The ML estimator deteriorates rapidly with phase error, due to the contributions of large (previously zero) terms in the summation expression for ML. The ML estimator fails completely when the random phase error is greater than 30 deg. The RML estimator avoids this problem by omitting the destabilizing terms from the summation. The terms remaining in the RML summation are also affected by the introduction of phase errors, but to a much lesser extent. The RML estimator continues to perform accurately and reliably up to a random phase error of 85 deg.

ACKNOWLEDGMENTS

The authors would like to acknowledge several helpful discussions with George Frichter and Dr. George Smith during the course of this work. This work was supported by the Office of Naval Research, through Contract N00014-87-K-0394, and by the Naval Ocean Research and Development Activity.

APPENDIX A: FORMULATION OF $\mathbf{p}=U_s$: LOCAL NORMAL-MODE MODEL

In Sec. I we discussed the normal-mode model for propagation and showed that the single snapshot (narrow-band) data vector corresponding to a single source had the form $\mathbf{p} = U_s$, where the $N \times M$ matrix U is independent of the source and depends only on the array and the acoustic environment. All source dependencies are in the vector s, whose entries are given in Eq. (3). However, the typical normal-mode approach has the deficiency of being valid only for depth-dependent media, and does not permit inclusion of range dependencies. In this Appendix we shall show that the $\mathbf{p} = U_s$ formulation and preceding results are valid for complicated environments where the ocean channel has sound speed and density exhibiting both range and depth dependencies, as well as a rough surface. Such assumptions in modeling an ocean channel can be included in an extension of the normal-mode method to obtain solutions in terms of "local" normal modes. We shall use well-known methods[11,21] in deriving solutions. First we incorporate density changes into effective sound speed profiles, and then we obtain solutions in terms of orthogonal eigenfunctions and coupled modal amplitudes.

Consider a sound source positioned below the origin of a cylindrical coordinate system on the z axis at $z = z_s$. Assuming a cylindrically symmetric ocean channel, the surface is at

$Z = d(r)$, and the bottom of the ocean sediments is at $z = D$. The ocean is assumed to have range- and depth-dependent sound speed $c(r,z)$ and density $\rho_0(r,z)$. Let the acoustic pressure be $p(r,z,t)$. Assuming harmonic time dependence with frequency ω radians per second, we have

$$p(r,z,t) = P(r,z)e^{-i\omega t}. \tag{A1}$$

We suppress any time dependence in the surface [choosing to view $d(r)$ as a member of an ensemble of random functions remaining fixed in source–receiver travel times] and hence also in P, which will satisfy the differential equation

$$\rho_0\nabla\cdot(\rho_0^{-1}\nabla P) + k^2 P = [-\delta(r)\cdot\delta(z-z_s)]/2\pi r, \tag{A2}$$

along with the horizontal boundary conditions,

$$P(r,d(r)) = 0 \tag{A3}$$

and

$$\frac{\partial P}{\partial z}(r,D) = 0. \tag{A4}$$

Equation (A3) corresponds to a pressure release surface, while Eq. (A4) is descriptive of a perfectly hard subbottom. In Eq. (A2), $k = \omega/c$ is the local wavenumber. By defining[11,13]

$$P(r,z) = \sqrt{\rho_0(r,z)}\,P'(r,z), \tag{A5}$$

and using Eq. (A2), P' satisfies

$$\nabla^2 P' + k_c^2 P' = [-\delta(r)\cdot\delta(z-z_s)]/2\pi r\rho_0, \tag{A6}$$

where

$$k_c^2 = k^2 + \tfrac{1}{2}\rho_0^{1/2}\nabla\cdot(\rho_0^{-3/2}\nabla\rho_0) \tag{A7}$$

is an effective local wavenumber. Hence, by defining an "effective" sound speed, $c_e = \omega/k_c$, one may implement density variations in numerical routines via effective sound speed profiles and modified source strength.

To derive coupled modes we let[11,21]

$$P'(r,z) = \sum_{n=1}^{\infty}\Phi_n(r)\Psi_n(z;r), \tag{A8}$$

where $\Psi_n(z;r)$ are solutions to the local normal-mode problems

$$\frac{\partial^2\Psi_n}{\partial z^2} + [k_c^2(r,z) - \kappa_n^2(r)]\,\Psi_n = 0, \tag{A9}$$

with

$$\Psi_n(d(r);r) = 0 \tag{A10}$$

and

$$\frac{\partial}{\partial z}(\rho_0^{-1}\Psi_n)_{z=D} = 0. \tag{A11}$$

See Ref. 11 for the equations that uniquely determine the Φ_n.

Now, if we use the typical definition for the vector

$$\mathbf{p} = [P(r,z_1),P(r,z_2),P(r,z_3),\ldots,P(r,z_N)]^T, \tag{A12}$$

and assume only a finite number (M) of modes propagate, then $\mathbf{p} = U_s$, where U is an $N\times M$ matrix with entries

$$U_{nm} = \sqrt{\rho_0(r,z_n)}\,\Psi_m(z_n;r), \quad \begin{matrix} n = 1,2,\ldots,N, \\ m = 1,2,\ldots,M, \end{matrix} \tag{A13}$$

and where $\mathbf{s}$ is a source dependent vector with the M components

$$s_m = \Phi_m(r), \quad m = 1,2,\ldots,M. \tag{A14}$$

Note that the s_m depend on source range and depth. In the case when there is modal and white noise, in addition to a particular signal of interest, one writes

$$\mathbf{x} = U_s + U\gamma + \eta, \tag{A15}$$

as in Eq. (1). Even though it appears that Eq. (A13) depends on source range (since that is where the origin is positioned) it is actually not dependent on the distance between the source and receiver but on the actual location of the receiver; i.e., for different source locations the U_{mn} are still the same.

APPENDIX B: FORMULATION OF $\mathbf{p}=U_s$: PARABOLIC APPROXIMATION MODEL

For actual applications, the system of equations in the preceding appendix may be quite difficult to solve. The Parabolic Approximation method simplifies the modal amplitude equations. If, instead of using Eq. (A5), one uses the assumption[13] that

$$P(r,z) = \sqrt{\rho_0(r,z)}\,u(r,z)H_0^{(1)}(k_0 r), \tag{B1}$$

where in the farfield

$$H_0^{(1)}(k_0 r) \sim \sqrt{2/i\pi k_0 r}\,e^{ik_0 r}, \quad k_0 r \gg 1, \tag{B2}$$

then, away from the source, $u(r,z)$ satisfies the parabolic approximation

$$\frac{\partial^2 u}{\partial z^2} + 2ik_0\frac{\partial u}{\partial r} + [k_c^2(r,z) - k_0^2]\,u = 0, \tag{B3}$$

where $k_0 = \omega/c_0$ is a reference wavenumber and c_0 is a reference sound speed. Now if one writes

$$u(r,z) = \sum_{n=1}^{\infty}\Gamma_n(r)\Psi_n(z;r), \tag{B4}$$

with Ψ_n determined as in Eqs. (A9)–(A11), then Γ_n will be solutions of

$$\frac{d\Gamma_n}{dr} - \frac{i}{2k_0}[\kappa_n^2(r) + k_0^2]\,\Gamma_n = -\sum_{m=1}^{\infty}A_{nm}(r)\Gamma_m, \tag{B5}$$

where A_{nm} are integral functions of Ψ_n and Ψ_m, given in Ref. 11.

If $\mathbf{a}$ is a vector of length M whose components are modal amplitudes Γ_n, and if we approximate the solution by assuming M modes propagate, then $\mathbf{a}$ satisfies the first-order problem

$$\mathbf{a}' = \Omega(r)\mathbf{a}, \tag{B6}$$

where Ω is an $M\times M$ matrix with entries

$$\Omega_{nm} = \begin{cases} \dfrac{i}{2k_0}(\kappa_n^2 + k_0^2) - A_{mm}(r), & m = n, \\ -A_{nm}(r) & m \neq n. \end{cases} \tag{B7}$$

Hence, if $\exp[\int_0^r\Omega(\tau)\,d\tau]$ is the matrix exponential corresponding to the integral of Ω then one can write

$$\mathbf{a} = \exp\left(\int_{r_0}^{r} \Omega(\tau)\, d\tau\right)\mathbf{c}\,, \tag{B8}$$

where $\mathbf{c}$ is a constant vector determined by the initial condition.

The advantage to this method is that determination of the matrix exponential in Eq. (B8) is perhaps easier than solving the system of coupled equations in the previous formulation. In this case, the $\mathbf{p} = U\mathbf{s}$ is still valid, with

$$\mathbf{s} = \mathbf{a}H_0^{(1)}(k_0 r)\,. \tag{B9}$$

It is important to again note that U is only dependent upon receiver locations and the particular ocean characteristics at the receiving array, while $\mathbf{s}$ contains all source information.

APPENDIX C: ESTABLISHING THE ML ESTIMATE WHEN $R = UU^H$

To establish the existence of the limit of the denominator of the maximum likelihood estimator [i.e., $\mathbf{p}(r,z)^H(UU^H + \epsilon I)^{-1}\mathbf{p}(r,z)$] as $\epsilon \to 0$ we first write

$$(UU^H + \epsilon I)U = U(U^H U + \epsilon I)\,, \tag{C1}$$

from which it follows that

$$(UU^H + \epsilon I)^{-1}U = U(U^H U + \epsilon I)^{-1}\,. \tag{C2}$$

Now we write the denominator of the ML estimator as $\mathbf{p}(r,z)^H(UU^H + \epsilon I)^{-1}\mathbf{p}(r,z)$ and using the relation $\mathbf{p}(r,z) = U\mathbf{s}(r,z)$ we have

$$\begin{aligned}&\mathbf{p}(r,z)^H(UU^H + \epsilon I)^{-1}\mathbf{p}(r,z)\\ &\quad = \mathbf{s}(r,z)^H U^H(UU^H + \epsilon I)^{-1}U\mathbf{s}(r,z)\,,\end{aligned} \tag{C3}$$

and using (C1) we find

$$\begin{aligned}&\mathbf{p}(r,z)^H(UU^H + \epsilon I)^{-1}\mathbf{p}(r,z)\\ &\quad = \mathbf{s}(r,z)^H U^H U(U^H U + \epsilon I)^{-1}\mathbf{s}(r,z)\\ &\quad = \mathbf{s}(r,z)^H(U^H U + \epsilon I)(U^H U + \epsilon I)^{-1}\mathbf{s}(r,z)\\ &\qquad - \epsilon\mathbf{s}(r,z)^H(U^H U + \epsilon I)^{-1}\mathbf{s}(r,z)\\ &\quad = \mathbf{s}(r,z)^H\mathbf{s}(r,z) - \epsilon\mathbf{s}(r,z)^H(U^H U + \epsilon I)^{-1}\mathbf{s}(r,z)\,.\end{aligned} \tag{C4}$$

Since $\mathbf{s}(r,z)^H(U^H U + \epsilon I)^{-1}\mathbf{s}(r,z)$ goes to $\mathbf{s}(r,z)^H(U^H U)^{-1}\mathbf{s}(r,z)$ as ϵ goes to zero, it follows that the entire expression goes to $\mathbf{s}(r,z)^H\mathbf{s}(r,z)$.

[1] H. Bucker, "Use of calculated sound fields and matched field detection to locate sound sources in shallow water," J. Acoust. Soc. Am. **59**, 368–373 (1976).

[2] A. Baggeroer, W. Kuperman, and H. Schmidt, "Matched field processing: Source localization in correlated noise as an optimum parameter estimation problem," J. Acoust. Soc. Am. **83**, 571–587 (1988).

[3] M. B. Porter, R. L. Dicus, and R. G. Fizell, "Simulations of matched field processing in a deep-water Pacific environment," IEEE J. Oceanic Eng. **OE-12**, 173–181 (1987).

[4] E. C. Shang, "Source depth estimation in waveguides," J. Acoust. Soc. Am. **77**, 1413–1418 (1985).

[5] T. C. Yang, "A method of range and depth estimation by modal decomposition," J. Acoust. Soc. Am. **82**, 1736–1745 (1987).

[6] J. Capon, "High resolution frequency-wavenumber spectrum analysis," Proc. IEEE **87**, 1408–1418 (1969).

[7] R. T. Lacoss, "Data adaptive spectral analysis methods," Geophysics **36**, 661–675 (1971).

[8] C. Byrne and A. Steele, "Sector focused stability for high resolution array processing," IEEE Proc. ICASSP-87, 2340–2342 (1987).

[9] M. Buckingham, "A theoretical model of ambient noise in a low-loss, shallow water channel," J. Acoust. Soc. Am. **67**, 1186–1192 (1980).

[10] W. A. Kuperman and F. Ingenito, "Spatial correlation of surface generated noise in a stratified ocean," J. Acoust. Soc. Am. **67**, 1988–1996 (1980).

[11] C. A. Boyles, *Acoustic Waveguides: Applications to Oceanic Science* (Wiley, New York, 1984).

[12] C. A. Boyles, "Coupled mode solution for a cylindrically symmetric oceanic waveguide with a range and depth dependent refractive index and a time varying rough sea surface," J. Acoust. Soc. Am. **73**, 800–805 (1983).

[13] F. D. Tappert, "The Parabolic Approximation Method" in *Wave Propagation in Underwater Acoustics*, edited by J. Keller and J. Papadakis (Springer, New York, 1977), pp. 224–284.

[14] M. Buckingham, "Array gain of a broadside vertical line array in shallow water," J. Acoust. Soc. Am. **65**, 148–161 (1979).

[15] G. Strang, *Linear Algebra and its Applications* (Academic, Orlando, 1980), 2nd ed., (a) pp. 84–89; (b) p. 131.

[16] C. L. Pekeris, "Theory of propagation of explosive sound in shallow water," Geol. Soc. Am. Mem. **27**, 43–64 (1948).

[17] L. E. Kinsler, A. R. Frey, A. B. Coppens, and J. V. Saunders, *Fundamentals of Acoustics* (Wiley, New York, 1982), 3rd ed., pp. 434–440.

[18] C. Feuillade and W. A. Kinney, "Source localization using a matched-field technique," J. Acoust. Soc. Am. Suppl. 1 **78**, S30 (1985).

[19] G. S. Smith, C. Feuillade, D. R. DelBalzo, and C. L. Byrne, "A non-linear matched-field processor for detection and localization of a quiet source in a noisy shallow-water environment," J. Acoust. Soc. Am. **85**, 1158–1166 (1989).

[20] C. Feuillade, D. R. DelBalzo and M. M. Rowe, "Environmental mismatch in shallow-water matched-field processing: geoacoustic parameter variability," J. Acoust. Soc. Am. **85**, 2354–2364 (1989).

[21] A. D. Pierce, *Acoustics: An Introduction to its Physical Principles* (McGraw-Hill, New York, 1981).